Effect of lateral fluoro substituents on the chiral liquid crystal materials derived from (*S*)-1-methyl-2-(2'-methylsulphanylethoxy)ethanol

Mei-Ching Yu[a]; Hau-Yun Chang[a]; Shune-Long Wu[a]

[a] Department of Chemical Engineering, Tatung University, Taipei, 104, Taiwan, ROC

PLEASE SCROLL DOWN FOR ARTICLE

Taylor & Francis
Taylor & Francis Group

Effect of lateral fluoro substituents on the chiral liquid crystal materials derived from (*S*)-1-methyl-2-(2′-methylsulphanylethoxy)ethanol

MEI-CHING YU, HAU-YUN CHANG and SHUNE-LONG WU*

Department of Chemical Engineering, Tatung University, 40 Chungshan N. Rd., 3rd Sec., Taipei, 104, Taiwan, ROC

Two series of chiral materials, the (*R*)-1-methyl-2-(2′-methylsulphanylethoxy)ethyl 4-(4′-alkoxybiphenyl-1-carboxyloxy)-2-fluorobenzoates, 2F3H(*m*=7–10), and the (*R*)-1-methyl-2-(2′-methylsulphanylethoxy)ethyl 4-(4′-alkoxybiphenyl-1-carboxyloxy)-3-fluorobenzoates, 2H3F(*m*=7–10), were synthesized for investigation. Polymorphism of the materials was detected primarily by polarizing microscopy and differential scanning calorimetry. The ferroelectric and antiferroelectric phases were further characterized by switching current behaviour, electro-optical response and dielectric permittivity. The results show that the antiferroelectric SmC_A^* phase occurred in two materials, 2F3H(*m*=7) and 2H3F(*m*=8). The spontaneous polarization and apparent tilt angle for the materials in the SmC* and/or SmC_A^* phases were also measured. The effect of fluoro substituents on the physical properties of the materials is discussed.

1. Introduction

A previous study on a homologous series of chiral liquid crystal materials, the (*R*)-1-methyl-2-(2′-methylsulphanylethox)ethyl 4-(4′-alkoxybiphenyl-1-carboxyloxy)-benzoates, 2H3H(*m*), showed that the materials possess an antiferroelectric SmC_A^* phase in the shorter achiral alkyl chain members, 2H3H(*m*=7–9). This series of materials is structurally similar to MHPOBC; the first reported antiferroelectric liquid crystal material, which was found to posses fast response and tristable switching properties and has potential for the display devices [1]. The development of this type of the material has therefore become a significant topic in the field of liquid crystals. In order to explore further, two series of lateral fluoro-substituted derivatives of 2H3H(*m*), 2F3H(*m*) and 2H3F(*m*) whose structural formulas are shown in scheme 1, were prepared for the investigation of mesomorphic and electro-optical properties.

Fluorine atoms have often been included as lateral substituents on the mesogenic core of liquid crystal molecules [2–9]. This incorporation has been found to cause some degree of steric asymmetry when the molecules are packed together, it therefore reduces the occurrence of higher order smectic phase, and decreases the melting point in most cases [10]. Other reports have indicated that the introduction of a lateral fluoro

substituent into mesogenic cores can enhance the formation of a tilted smectic C phase [8, 11, 12].

2. Experimental

2.1. *Characterization of materials*

The structures of intermediates and final products were checked by thin layer chromatography and further identified by nuclear magnetic resonance spectroscopy using a Bruker Avance 500 NMR spectrometer. The purity of the final products was confirmed by elemental analysis using a Perkin-Elmer 2400 instrument. The carbon and hydrogen analytical data agreed with calculated results within $\pm 1\%$.

Phase transition temperatures and enthalpy changes were determined by differential scanning calorimetry (DSC) using a Perkin-Elmer DSC 7 at a running rate of $5°C\,min^{-1}$. Mesophases were identified using a Nikon Microphot-FXA polarizing optical microscope in conjunction with a Mettler FP82-HT hot stage controlled by a Mettler FP90 processor.

Commercial homogenous cells coated with polyimide as alignment film were purchased from E.H.C. Co. Ltd, Japan and Linkam Scientific Instruments Ltd, UK. The sample was filled into the cell by capillary action in the isotropic state. Two wires were fixed separately with silver paint to the ITO-coated glass plates of the sample cell.

Spontaneous polarization (P_s) was measured by the triangular wave method [13]. Triangular waves were generated by a Yogawa AG1200 arbitrary waveform generator
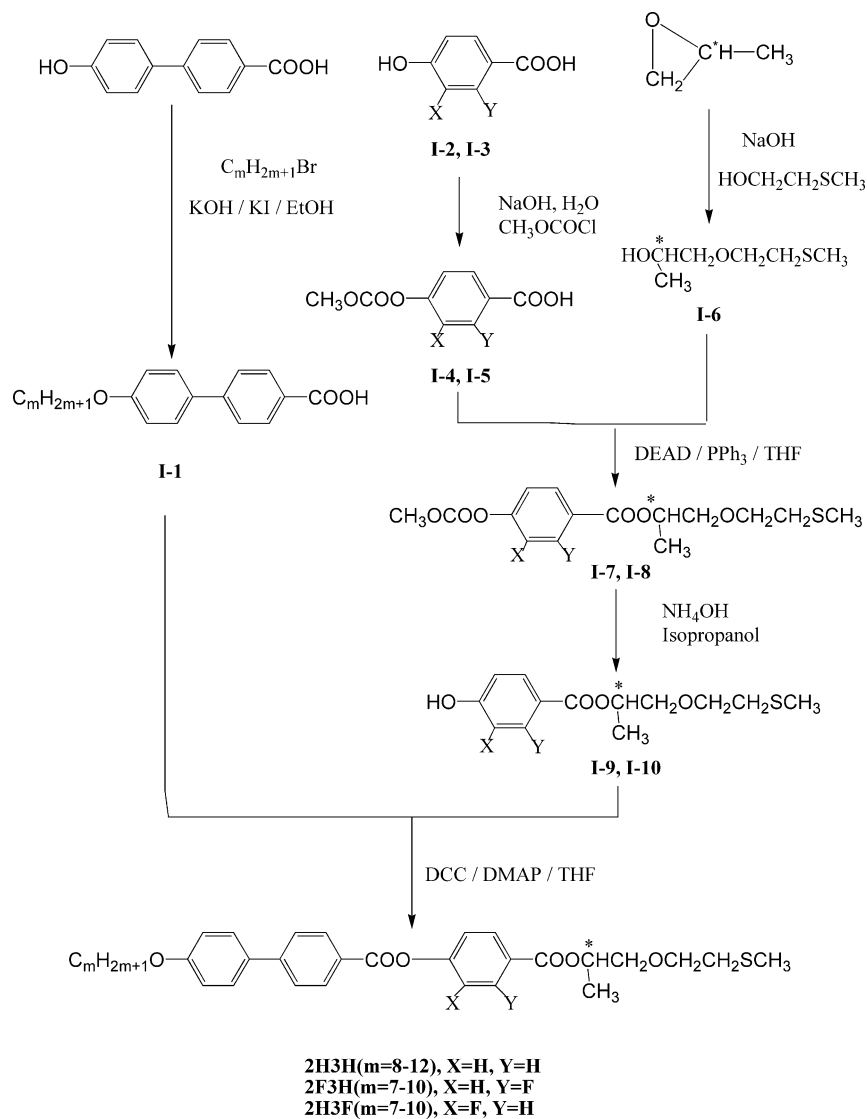
Scheme.   Schematic procedures for the synthesis of the chiral materials.

and were amplified by an NF Electronics Instrument 4005 power amplifier. The currents were measured by detecting the voltage change across a resistor of $50\,k\Omega$, using a HP 4284A digital oscilloscope to monitor the signals.

The measurement of optical transmittance versus applied electric field was conducted using a He–Ne laser ($5\,mW$, $632.8\,nm$) as probe beam [14, 15]. The optical transmittance of the probe beam passing through the cell, between crossed polarizers with axes parallel and perpendicular to the smectic layer normal, was detected by a photodiode.

2.2.   Preparation of materials

The starting chiral material, (*S*)-propylene oxide, was purchased from Sigma-Aldrich Chemie GmbH P.O.,

with purity greater than 99%. Thin layer chromatography was performed with TLC sheets coated with silica; spots were detected by UV irradiation. Silica gel (MN kieselgel 60, 70–230 mesh) was used for column chromatography. The organic solvent dichloromethane (CH_2Cl_2) and tetrahydrofuran (THF), were purified by treatment with CaH_2 and $LiAlH_4$, respectively, and distilled before use. A summary of the synthesis procedure is shown in scheme 1.

2.2.1.   2-Fluoro-4-hydroxybenzoic acid, I-2.
2-Fluoro-4-methoxycarbonyloxybenzoic acid was prepared according to the method previously described [16, 17]. ^{1}H NMR (500 MHz, DMSO-d_6): δ(ppm) 3.84–3.87 (s, 3H, –OCH$_3$), 7.16–7.23 (d, 1H, –ArH, $J=6.7\,Hz$), 7.31–7.38

(d, 1H, –Ar**H**, *J*=9.4 Hz), 7.91–7.95 (t, 1H, –Ar**H**, *J*= 8.5 Hz), 9.15 (s, 1H, –COO**H**).

2.2.2. 3-fluoro-4-hydroxybenzoic acid, I-3. 3-Fluoro-4-methoxycarbonyloxybenzoic acid was prepared as previously described [18–22]. ^{1}H NMR (500 MHz, DMSO-d$_6$): *δ*(ppm) 3.96 (s, 3H, –OC**H**$_3$), 7.34–7.37 (t, 1H, –Ar**H**, *J*=7.4 Hz), 7.91–7.93 (d, 1H, –Ar**H**, *J*= 9.8 Hz), 7.93–7.94 (t, 1H, –Ar**H**, *J*=6.1 Hz), 9.03 (s, 1H, –COO**H**).

2.2.3. 2-fluoro4-methoxycarbonyloxybenzoic acid, I-4. To a solution of sodium hydroxide (7.5 g, 175 mmol) in water (200 ml) which was maintained at 0°C, 4-hydroxybenzoic acid (9 g, 65 mmol) was added with vigorous stirring, Methyl chloroformate (10 g, 105 mmol) was then added slowly to the resulting suspension which was maintained at 0–5°C. The resulting slurry was stirred for a further 4 h and brought to pH=5 by the addition of conc. hydrochloric acid and water (1:1). The voluminous precipitate was filtered off and recrystallized from ethanol to give **I-4** as a white solid; yield 84%, m.p. 173–176°C. ^{1}H NMR (500 MHz, CDCl$_3$): *δ*(ppm) 1.36–1.60 (d, 3H, –CH*C**H**$_3$, *J*=8.4 Hz), 3.75–3.96 (m, 2H, –CH*C**H**$_2$OCH$_2$–), 3.92–3.93 (s, 3H, –OCOOC**H**$_3$, *J*=6.5 Hz), 3.95–3.98 (m, 2H, –CH$_2$OCH$_2$CF$_2$–), 5.29–5.36 (m, 1H, –COOC**H***CH$_3$), 7.25–7.27 (d, 2H, Ar**H**, *J*=8.8 Hz), 8.05–8.08 (t, 1H, Ar**H**, *J*=8.7 Hz).

2.2.4. 3-Fluoro-4-methoxycarbonyloxybenzoic acid, I-5. This material was prepared in an analogous manner to **I-4**; the yield was 80%. ^{1}H NMR (500 MHz, CDCl$_3$): *δ*(ppm) 1.37–1.60 (d, 3H, –CH*C**H**$_3$, *J*=8.2 Hz) 3.96 (s, 3H, –OC**H**$_3$), 5.28–5.37 (m, 1H, –COOC**H***CH$_3$), 7.34–7.37 (t, 1H, –Ar**H**, *J*=7.4 Hz), 7.91–7.93 (d, 1H, –Ar**H**, *J*=8.8 Hz).

2.2.5. (S)-[1-Methyl-2-(2′-methylsulphanylethoxy)]ethanol, I-6. 2-(Methylsulphanyl)-1-ethanol (25.4 g, 275 mmol) and sodium hydroxide (0.1 g, 2.5 mmol) were heated under reflux for 2 h and cooled to room temperature; (S)-propylene oxide (8.0 g, 13.8 mmol) was added dropwise and the mixture heated under reflux overnight. After filtering, excess 2-(methylsulphanyl)-1-ethanol was removed under vacuum. The resinous mass thus obtained was distilled under high vacuum to give a 63% yield of pure product, b.p. 88°C/22 torr. ^{1}H NMR (500 MHz, CDCl$_3$): *δ*(ppm) 1.15–1.16 (d, 3H, –C*HC**H**$_3$CH$_2$O–), 2.16 (s, 3H, –CH$_2$CH$_2$S–C**H**$_3$), 2.51 (s, 1H, –O**H**), 2.70–2.72 (t, 2H, –C**H**$_2$CH$_2$SCH$_3$), 3.24–3.50 (m, 2H, –C**H**$_2$OCH$_2$CH$_2$S–), 3.64–3.72 (m, 2H, –CH$_2$C**H**$_2$SCH$_3$), 3.96–4.00 (m, 1H, –C*HC**H**$_3$COO–).

2.2.6. (R)-[1-Methyl-2-(2′-methylsulphanylethoxy)]ethyl 4-(methoxycarbonyloxy)-2-fluorobenzoate, I-7. A solution of diethyl azodicarboxylate (1.50 g, 8.61 mmol) and compound **I-4** (1.18 g, 7.85 mmol) in anhydrous THF (10 ml) was added dropwise to a solution of triphenylphosphine (2.27 g, 8.65 mmol) and compound **I-6** (1.86 g, 8.65 mmol) in anhydrous THF (10 ml) at room temperature with vigorous stirring; the reaction soon started. After standing overnight at room temperature, triphenylphosphine oxide was removed by filtration and the THF was removed under vacuum. After the work-up procedure, the product was isolated by column chromatography over silica gel (70–230 mesh) using ethyl acetate/hexane (v/v=1/4) as eluant, to give a colourless liquid in 65% yield. ^{1}H NMR (500 MHz, CDCl$_3$): *δ*(ppm) 1.36–1.37 (d, 3H, –C*HC**H**$_3$CH$_2$O–), 2.13 (s, 3H, –CH$_2$CH$_2$SC**H**$_3$), 2.65–2.68 (t, 2H, –C**H**$_2$CH$_2$SCH$_3$), 3.58–3.68 (m, 2H, –C**H**$_2$OCH$_2$CH$_2$S–), 3.70–3.73 (m, 2H, –CH$_2$C**H**$_2$SCH$_3$), 3.92 (s, 3H, C**H**$_3$OCOO–), 5.29–5.35 (m, 1H, –C*HC**H**$_3$COO–), 7.25–7.26 (d, 2H, –Ar**H**), 8.07–8.09 (d, 2H, –Ar**H**).

2.2.7. (R)-[1-Methyl-2-(2′-methylsulphanylethoxy)]ethyl 4-(methoxycarbonyloxy)-3-fluorobenzoate, I-8. This material was prepared in an analogous manner to **I-7**; the yield was 78%. ^{1}H NMR (500 MHz, CDCl$_3$): *δ*(ppm) 1.36–1.37 (d, 3H, –C*HC**H**$_3$CH$_2$O–), 2.14 (s, 3H, –CH$_2$CH$_2$SC**H**$_3$), 2.65–2.67 (t, 2H, –C**H**$_2$CH$_2$SCH$_3$), 3.60–3.69 (m, 2H, –C**H**$_2$OCH$_2$CH$_2$S–), 3.71–3.75 (m, 2H, –CH$_2$C**H**$_2$SCH$_3$), 3.94 (s, 3H, C**H**$_3$OCOO–), 5.30–5.34 (m, 1H, –C*HC**H**$_3$COO–), 7.25–7.26 (d, 2H, –Ar**H**), 8.05–8.09 (d, 2H, –Ar**H**).

2.2.8. (R)-1-Methyl-2-(methylsulphanyl)ethyl 4-hydroxy-2-fluorobenzoate, I-9. Compound **I-7** (1.61 g, 4.64 mmol) was stirred in a mixture of isopropanol (70 ml) and ammonia (28%, 20 ml) at room temperature for 50 min (TLC analysis showed a complete reaction) and then poured into water (40 ml) with stirring. The product was extracted with dichloromethane (3 × 50 ml). The combined organic extracts were washed with brine (3 × 50 ml), dried (MgSO$_4$), filtered and evaporated to give a colourless oil. The oil was purified by column chromatography over silica gel (70–230 mesh) using dichloromethane as eluant. The isolated product was then dried in vacuo; 90% yield of product was obtained. ^{1}H NMR (500 MHz, CDCl$_3$): *δ*(ppm) 1.34–1.36 (d, 3H, –C*HC**H**$_3$CH$_2$O–), 2.12 (s, 3H, –CH$_2$CH$_2$SC**H**$_3$), 2.66–2.69 (t, 2H, –C**H**$_2$CH$_2$SCH$_3$), 3.58–3.69 (m, 2H, –C**H**$_2$OCH$_2$CH$_2$S–), 3.71–3.75 (m, 2H, –CH$_2$C**H**$_2$SCH$_3$), 4.69 (s, 1H, –O**H**), 5.27–5.32 (m, 1H, –C*HC**H**$_3$COO–), 6.84–6.86 (d, 2H, –Ar**H**), 7.92–7.94 (d, 2H, –Ar**H**).

2.2.9. (*R*)-1-Methyl-2-(methylsulphanyl)ethyl 4-hydroxy-2-fluorobenzoate, I-10. This material was prepared in an analogous manner to **I-9**; the yield was 88%. ^{1}H NMR (500 MHz, CDCl$_3$): δ(ppm) 1.33–1.34 (d, 3H, –C*H**CH$_3$**CH$_2$O–), 2.12 (s, 3H, –CH$_2$CH$_2$S**CH$_3$**), 2.68–2.69 (t, 2H, –CH$_2$**CH$_2$**SCH$_3$), 3.60–3.69 (m, 2H, –C**H$_2$**OCH$_2$CH$_2$S–), 3.71–3.73 (m, 2H, –CH$_2$**CH$_2$**SCH$_3$), 4.70 (s, 1H, –O**H**), 5.24–5.32 (m, 1H, –C*H**CH$_3$**COO–), 6.84–6.86 (d, 2H, –Ar**H**), 7.94–7.97 (d, 2H, –Ar**H**).

2.2.10. (*R*)-[1-Methyl-2-(2′-methylsulfanylethoxy)]ethyl 4-(4′-alkoxybiphenyl-1-carboxyloxy)-2-fluorobenzoates, 2F3H(*m*=7–10). A mixture of a 4-(4′-alkyloxyphenyl)-benzoic acid (2.54 mmol), compound **I-7** (0.76 g, 2.62 mmol), *N*,*N*-dicyclohexylcarbodiimide (0.35 g, 2.8 mmol), 4-dimethylaminopyridine (0.06 g, 0.28 mmol) and dry THF (15 ml) was stirred at room temperature for three days. The precipitate was filtered off and the filtrate washed with 5% acetic acid solution (3×50 ml), 5% saturated aqueous sodium hydrogen carbonate (3×50 ml) and water (3×50 ml); the filtrate was then dried over anhydrous magnesium sulphate (MgSO$_4$) and concentrated in vacuum. The residue was purified by column chromatography over silica gel (70–230 mesh) using dichloromethane as eluant. The products were crystallized from absolute ethanol and yielded 50% of pure compound. Typical data for **2F3H(*m*=10)**, as example: ^{1}H NMR (500 MHz, CDCl$_3$): δ(ppm) 0.87–0.90 (t, 3H, **CH$_3$**(CH$_2$)$_4$–), 1.24–1.59 (m, 8H, –CH$_3$(**CH$_2$**)$_4$–), 2.04–2.14 (s, 3H, –CH$_2$CH$_2$S**CH$_3$**), 2.67–2.70 (t, 2H, –CH$_2$**CH$_2$**SCH$_3$), 3.60–3.76 (m, 4H, –C**H$_2$**OC**H$_2$**CH$_2$S–), 3.73–3.76 (m, 2H, –CH$_2$**CH$_2$**SCH$_3$), 4.00–4.03 (t, 2H, C**H$_2$**CH$_2$O–), 5.35–5.36 (m, 1H, –C*H**CH$_3$**COO–), 7.00–7.01 (d, 2H, –Ar**H**), 7.31–7.33 (d, 2H, –Ar**H**), 7.59–7.61 (d, 2H, –Ar**H**), 7.69–7.71 (d, 2H, –Ar**H**), 8.13–8.14 (d, 2H, –Ar**H**), 8.22–8.24 (d, 2H, –Ar**H**).

2.2.11. (*R*)-[1-Methyl-2-(2′-methylsulphanylethoxy)]ethyl 4-(4′-alkoxybiphenyl-1-carboxyloxy)-3-fluorobenzoates, 2H3F(*m*=7–10). These materials were prepared in an analogous manner to **2H3F(*m*=7–10)**; the yields were 50%. Typical data for **2H3F(*m*=10)** as example: ^{1}H NMR (500 MHz, CDCl$_3$): δ(ppm) 0.87–0.90 (t, 3H, **CH$_3$**(CH$_2$)$_4$–), 1.25–1.58 (m, 8H, –CH$_3$(**CH$_2$**)$_4$–), 2.13–2.15 (s, 3H, –CH$_2$CH$_2$S**CH$_3$**), 2.67–2.70 (t, 2H, –CH$_2$**CH$_2$**SCH$_3$), 3.59–3.74 (m, 4H, –C**H$_2$**OC**H$_2$**CH$_2$S–), 3.73–3.76 (m, 2H, –CH$_2$**CH$_2$**SCH$_3$), 4.00–4.03 (t, 2H, –C**H$_2$**CH$_2$O–), 5.35–5.36 (m, 1H, –C*H**CH$_3$**COO–), 6.99–7.01 (d, 2H, Ar**H**), 7.31–7.33 (d, 2H, Ar**H**), 7.59–7.61 (d, 2H, Ar**H**), 7.69–7.71 (d, 2H, Ar**H**), 8.13–8.14 (d, 2H, –Ar**H**), 8.22–8.25 (d, 2H, Ar**H**).

All the target materials were analysed by elemental analysis for purity, with satisfactory results.

3. Results and discussion

3.1. *Mesophase properties*

The phase transitions and corresponding transition enthalpies of mesophases for the materials **2F3H(*m*= 7–10)** and **2H3F(*m*=7–10)** were observed by DSC. The mesophases were identified by the observation of microscopic textures under crossed polarizers. The SmC* and SmC$_A^*$ phases were further characterized by their switching behaviour and electro-optical response. The results are summarized in tables 1 and 2.

The phase charts are plotted in the figures 1 (*a*) and 1 (*b*) for comparison of the mesophases with respect to the achiral alkyl chain length *m* for both series of materials. It was found that 2-fluoro substituted materials have higher thermal stability in the ferroelectric SmC* phase than have the 3-fluoro substituted materials. Incorporation of lateral fluoro substituents in the 2-position of the phenyl ring of the molecules results in the formation of an enantiotropic SmC* phase; while that in the 3-position of the phenyl ring results in formation of a monotropic SmC* phase. Comparing fluoro-substituted materials with non-substituted materials, it is interesting to find that lateral fluoro substituents generally reduce the I–SmA* and SmA*–SmC* transition temperatures and melting points. Unlike the non-substituted materials **2H3H(*m*)**, where the antiferroelectric SmC$_A^*$ phase occurs for alkyl chain lengths *m*=7–9, these two series of fluoro substituted materials only have (a) an enantiotropic SmC$_A^*$ phase which appears in **2F3H(*m*=7)**, and (b) a monotropic

Table 1. Mesophases, transition temperatures (°C) and associated enthalpy data (kJ mol^{-1}, in parentheses) for the chiral materials **2F3H(*m*=7–10)**.

m	I		SmA*		SmC*		SmC$_A^*$		Cr	m.p.
7	•	126.03 (4.36)	•	100.31 (0.01)	•	76.05	•	23.41 (2.37)	•	62.16 (33.04)
8	•	123.64 (2.31)	•	100.88 (0.11)	•	[a]		5.29 (1.12)	•	10.73 (1.19)
9	•	119.18 (4.17)	•	100.05 (0.19)	•			1.56 (12.36)	•	41.18 (21.55)
10	•	117.59 (3.75)	•	100.53 (0.37)	•			9.58 (15.86)	•	48.53 (23.54)

[a]The enthalpy was too small to be determined by DSC.

Table 2. Mesophases, transition temperatures (°C) and associated enthalpy data (kJ mol^{-1}, in parentheses) for the chiral materials **2H3F(m=7–10)**.

m	I		SmA*		SmC*		SmC$_A^*$		Cr		m.p.
7	•	107.52 (9.02)	•					•	49.72 (20.43)	•	61.77 (32.14)
8	•	105.87 (8.82)	•	44.25 (0.13)	•	42.03	•	39.79 (21.52)	•	52.53 (24.62)
9	•	96.73 (8.46)	•	46.38 (0.16)	•	a		25.85 (29.39)	•	64.76 (51.76)
10	•	90.83 (5.65)	•	47.52 (0.43)	•			14.94 (19.54)	•	53.79 (39.62)

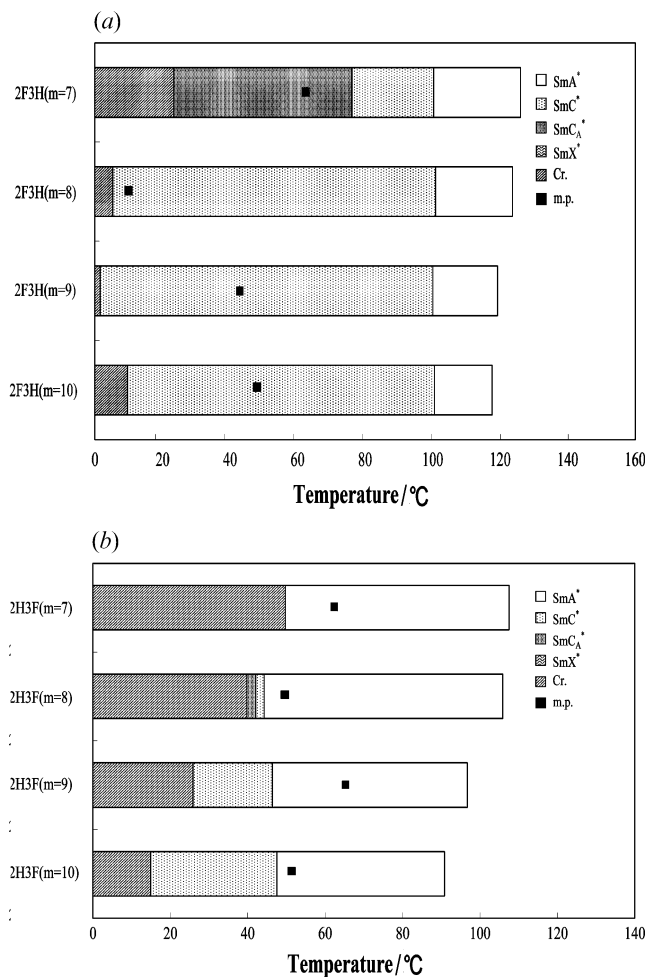[a]The enthalpy was too small to be determined by DSC.

(a)

(b)

Figure 1. Plot of transition temperature as a function of terminal alkyl chain length for the materials (a) **2F3H(m=7–10)** and (b) **2H3F(m=7–10)** during cooling.

SmC$_A^*$ phase which appears in **2H3F(m=8)**. Nevertheless, an unidentified higher ordered SmX* phase which occurred in the non-substituted materials was absent in the fluoro-substituted materials.

3.2. Electro-optical studies

The switching current behaviour of **2F3H(m=7–10)** and **2H3F(m=7–10)** was measured in 5 μm homogeneous

cells under a triangular wave voltage with a field frequency of 20 Hz and amplitude of 5 V; representative results are shown in figure 2. In the SmC* phase, the single switching peak produced by polarization reversal
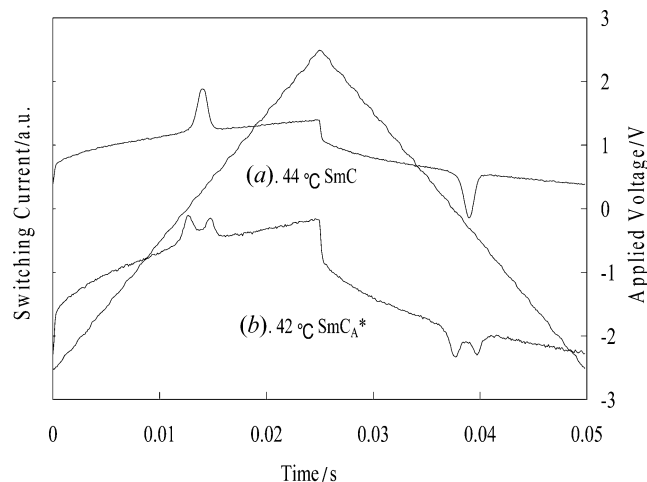

Figure 2. Switching current behaviour of material **2H3F(m=8)** obtained at 20 Hz and several temperatures on applying a triangular wave in a 5 μm thick homogeneously aligned cell.
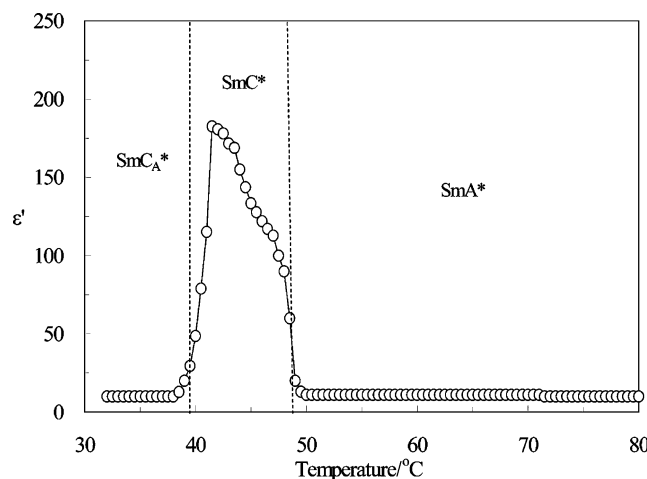

Figure 3. Temperature dependence of the dielectric constant ε' for the material **2H3F(m=8)**. The measurement was carried out at a cooling rate of 1°C min^{-1} and a frequency of 100 Hz.

of the charge suggests the existence of ferroelectricity [23]. In the SmC_A^* phase, two switching current peaks appeared, similar to the normal SmC_A^* phase [24], supporting the occurrence of antiferroelectricity.

Figure 3 shows the temperature dependence of the dielectric constants ε' for the material **2H3F(*m*=8)** measured at 100 Hz in 25 μm homogeneous cells. The ε' values in the SmA* phase are small, and the characteristic point corresponding to the SmA* to SmC* transition can be seen clearly. The great increase of dielectric constant on cooling to the SmC* phase is due to the contribution of the Goldstone mode. The dielectric constant falls to a very low value on further cooling from the SmC* phase to the SmC_A^* phase.
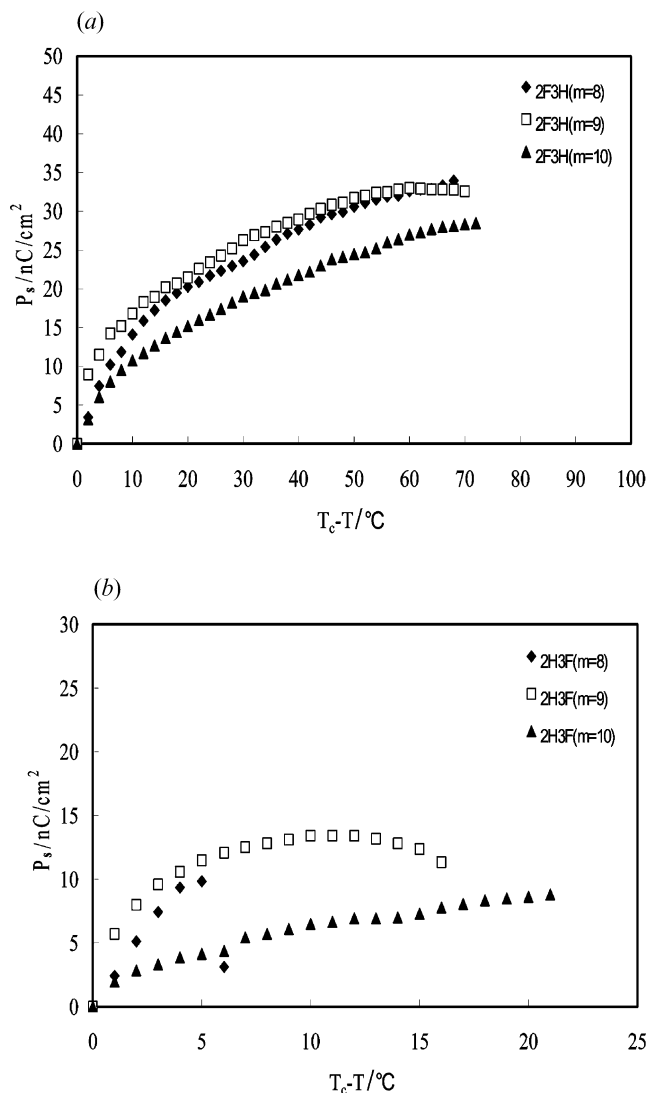

Figure 4. Spontaneous polarization plotted as a function of temperature for the materials (a) **2F3H(*m*=8–10)** and (b) **2H3F(*m*=8–10)**. The T_c is the temperature of the SmA*–SmC* transition.

The spontaneous polarizations (**P**$_s$) for compounds **2F3H(*m*=8–10)** and **2H3F(*m*=8–10)**, measured as a function of temperature on cooling in 5 μm homogeneous cells, are illustrated in figure 4. The **P**$_s$ values increase steeply in the vicinity of the SmA*–SmC* transition and then increase with decreasing temperature before crystallization. The maximum **P**$_s$ values measured from the materials **2F3H(*m*=8–10)** are in the range 28–34 nC cm^{-2}; those for **2H3F(*m*=8–10)** are in the range 5–14 nC cm^{-2}. Materials **2F3H(*m*=8–10)** show higher **P**$_s$ values than materials **2H3F(*m*=8–10)**. Materials **2H3H(*m*=8–10)** have maximum **P**$_s$ values higher than those of materials **2F3H(*m*=8–10)** and **2H3F(*m*=8–10)**, suggesting that the lateral fluoro subtituents suppress polarization, due to the transverse dipole of the fluoro atom in the phenyl ring of the molecule.

The temperature dependence of the optical tilt angle of the materials **2F3H(*m*=8–10)** and **2H3F(*m*=8–10)** was also measured, with the results shown in figure 5. The optical tilt angle increases dramatically as the
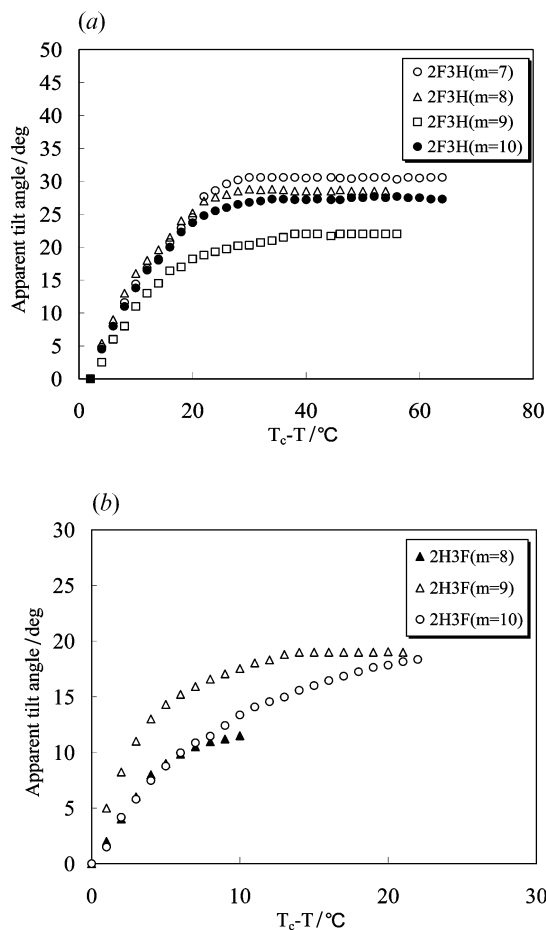

Figure 5. Temperature dependence of apparent tilt angles for the materials (a) **2F3H(*m*=8–10)** and (b) **2H3F(*m*=8–10)**.

temperature cooled from the SmA* phase region to the SmC* phase. The maximum optical tilt angles measured for the materials **2F3H(***m*=**8–10)** are in the range $20°$–$33.5°$; for **2H3F(***m*=**8–10)** they are in the range $10°$–$19.5°$. Materials **2F3H(***m*=**8–10)** have higher optical tilt angles than materials **2H3F(***m*=**8–10)**.

4. Conclusion

Two fluoro-substituted chiral materials, **2F3H(***m*=**7)** and **2H3F(***m*=**8)**, have been demonstrated to posses the antiferroelectric SmC_A^* phase. In general, fluoro substituents reduce the I–SmA* and SmA*–SmC* transition temperatures and melting points, and suppress the formation of a higher ordered SmX* phase. Incorporation of a fluoro substituent in the 2-position of the phenyl ring enhances the thermal stability of the ferroelectric SmC* phase, while a fluoro substituent in the 3-position suppresses its the thermal stability. The maximum P_s values and optical tilt angles in the SmC* phase of the chiral materials are also decreased by the introduction of fluoro substituents.

References

[1] A.D.L. Chandani, T. Hagiwara, Y. Suzuki, Y. Ouchi, H. Takezoe, A. Fukuda. *Jpn. J. appl. Phys.*, **27**, L126 (1988).
[2] V. Faye, C. Rouillon, C. Destrade, H.T. Nguyen. *Liq. Cryst.*, **19**, 47 (1995).
[3] C.D. Cruz, J.C. Rouillon, J.P. Marcerou, N. Isaert, H.T. Nguyen. *Liq. Cryst.*, **28**, 125 (2001).
[4] C.D. Cruz, J.C. Rouillon, J.P. Marcerou, N. Isaert, H.T. Nguyen. *Liq. Cryst.*, **28**, 1185 (2001).
[5] S. Essid, M. Manai, A. Gharbi, J.P. Marcerou, J.C. Rouillon, H.T. Nguyen. *Liq. Cryst.*, **31**, 1185 (2004).
[6] C.J. Booth, D.A. Dunmur, J.W. Goodby, J.S. Kang, K.J. Toyne. *J. mater. Chem.*, **4**, 747 (1994).
[7] C.C. Dong, M. Hird, J.W. Goodby. *Ferroelectrics*, **180**, 245 (1996).
[8] C.S. Hsu, C.H. Tsai. *Liq. Cryst.*, **22**, 669 (1997).
[9] S.L. Wu, C.Y. Lin. *Liq. Cryst.*, **30**, 471 (2003).
[10] D. Coates. *Liq. Cryst.*, **2**, 423 (1987).
[11] J.P. LePesant, J.N. Perbert, B. Mouret, M. Hareng, G. Decobert, J.C. Dubois. *Mol. Cryst. liq. Cryst.*, **129**, 61 (1985).
[12] S.M. Kelely. *Liq. Cryst.*, **2**, 423 (1989).
[13] K. Miyasato, S. Abe, H. Takezoe, A. Fukuda, T. Kuze. *Jpn. J. appl. Phys.*, **22**, L661 (1983).
[14] A.D.L. Chandani, T. Hagiwara, Y. Suzuki, Y. Ouchi, H. Takezoe, A. Fukuda. *Jpn. J. appl. Phys.*, **27**, L729 (1988).
[15] J. Lee, A.D.L. Chandani, K. Itoh, Y. Ouchi, H. Takezoe, A. Fukuda. *Jpn. J. appl. Phys.*, **29**, 1122 (1990).
[16] S.L. Wu, C.Y. Lin. *Liq. Cryst.*, **30**, 471 (2003).
[17] K. Miyasato, S. Abe, H. Takezoe, A. Fukuda, E. Kuze. *Jpn. J. appl. Phys.*, **22**, L661 (1983).
[18] M. Cepic, G. Heppke, J.M. Hollidt, D. Lotzsch, B. Beks. *Ferroelectrics*, **147**, 179 (1994).
[19] S.L. Wu, C.Y. Lin. *Liq. Cryst.*, **30**, 205 (2003).
[20] S.L. Wu, W.J. Hsieh. U.S. Patent 2 004 262 573 (2004).
[21] B. Kosata, J. Svoboda, V. Novotna, M. Glogarova. *Liq. Cryst.*, **31**, 1367 (2004).
[22] J.W. Goodby, P. Styring, C. Loubser, P.L. Wessels. UK Patent 19 941 214 (1994).
[23] C. Loubser, P.L. Wessels, P. Styring, J.W. Goodby. *J. mater. Chem.*, **4**, 71 (1994).
[24] M. Wand, R.R. Vohra, D. Walba. PCT Int. 19 920 206 (1992).